Resonance drifts of spiral waves on media of periodic excitability

Lida Xu,[1,2] Zhuang Li,[2,3] Zhilin Qu,[2] and Zengru Di[1,*]

[1]*Center for Complexity Research, Department of Systems Science, School of Management, Beijing Normal University, Beijing, 100875, China*

[2]*Department of Medicine (Cardiology), University of California, Los Angeles, California 90095, USA*

[3]*Mechanical Engineering College, Beijing Technology and Business University, Beijing, 100048, China*

(Received 25 January 2011; revised manuscript received 27 February 2012; published 24 April 2012)

Spiral waves subjected to an external periodic force exhibit very rich spatiotemporal dynamics including resonance attractors. In previous research, the modulation was mainly described as additional induced flow in the system, and a theory has been developed based on reducing the spiral wave dynamics to a low-dimensional map. In this paper, another perspective for study of the resonance attractors is suggested. The periodic modulation of excitability is directly described by the time dependence of the parameters. This approach gives us nice results that are well consistent with the experiments. Additionally, when we force the spiral with a frequency larger than its intrinsic frequency, another branch of spiral meandering with qualitatively different properties is observed. Full resonances are also clearly indicated. Furthermore, a kinetic model for spiral movement suggested in our previous paper is applied to this case. The theoretical results are in good quantitative agreement with numerical simulations. The model could be widely used in different excitable systems.

DOI: 10.1103/PhysRevE.85.046216 PACS number(s): 05.45.−a, 82.40.Ck, 47.32.C−, 89.75.−k

I. INTRODUCTION

Spiral waves are encountered in many kinds of excitable media; examples include the Belousov-Zhabotinsky (BZ) reaction [1,2], aggregating slime mold [3], the catalytic oxidation of CO on Pt [4], and effects in cardiac tissue [5–7]. They display many drift behaviors with different external fields, i.e., illumination [8], electric fields [9–14], and magnetic fields [15]. In particular, under external forcing by periodic light pulses and feedback-controlled sequences of light pulses, spiral wave entrainment and resonance can be observed [16,17]. In the feedback-controlled experiment, a spiral wave induced in the light-sensitive BZ system was disturbed by a sequence of short light pulses, which were applied immediately or after some time delay τ, corresponding to the passage of the wave front through a prechosen measuring point. Then the trajectory of the spiral wave tip represents a closed circular orbit around the measuring point [18]. Subsequent studies both experimental and theoretical revealed that the resonance attractor exhibits a complex structure with multiple orbits [19–21].

Actually, before the whole set of resonance attractors was observed in experiment [19], the above phenomenon had been theoretically studied [20]. Following the basic ideas proposed by Karma and Zykov [20], the theoretical analysis and numerical simulation are done mainly with the two-component Oregonator model, which is widely used to simulate the light-sensitive version of the BZ reaction:

$$\begin{aligned}\frac{\partial u}{\partial t} &= \nabla^2 u + \frac{1}{\varepsilon}\left[u - u^2 - (fv+\phi)\frac{u-q}{u+q}\right],\\ \frac{\partial v}{\partial t} &= u - v.\end{aligned} \tag{1}$$

The term $\phi = \phi(t)$ describes the additional bromide production that is induced by the external illumination of the system. When the function $\phi(t)$ presents as a sinusoidal form, this dynamic system will induce the spiral wave to undergo resonance drift. In Refs. [20,22], the authors found the dependence of the attractor radius R on the time delay τ by a kinematical analysis.

This consideration is based on the light-sensitive BZ system. The light pulses result in additional induced flow in the system and that can be described by the function $\phi(t)$ in Eq. (1). Actually, just as pointed out by Zykov *et al.* [17], the additional flow of the inhibitor Br^- will suppress the excitability of the medium (for instance, it decrease the propagation velocity of the excitation waves). So the illumination will finally affect the excitability of the medium. Thus the above experiments and phenomena could also be described by periodic disturbance of the excitability of the medium. The modulation of excitability provides us a more general perspective for investigating the effects of external forces. It has already been shown that parametric modulation of the excitability can induce very rich spatiotemporal dynamics of spiral waves. This approach could be applied to different kinds of excitable systems in addition to the light-sensitive BZ reaction.

In models of spiral wave dynamics, there are usually several parameters that govern the dynamics of the system. Although almost all the parameters are related to the medium excitability, the key parameter is the rate parameter ε. Thus in this paper, we suggest that a periodic change of the parameter ε can produce the same phenomenon of resonant drifting of the spiral wave. In fact, we have done the simulation with the Oregonator model given by Eq. (1). With periodic modulation of the parameter ε, the spiral wave given by the Oregonator model shows the same drifting behavior as that we present in this paper with the Barkley model. In the following discussion, to investigate how periodic modulation of the excitability of the medium can generate the same resonance drift of spiral waves, we use the Barkley model given by Eq. (2) to stimulate the experiment. The main reason is that, for the Barkley model, we already know the dependence of the core radius R_c and rotation period P_c on the parameter ε. Thus we can use the kinematic model to describe the drift dynamics.

*Author to whom correspondence should be addressed: zdi@bnu.edu.cn

Thus, in this paper, the sequence of short light pulses is described by corresponding changes of the parameter ε in the Barkley model. It may supply another reasonable explanation for the entrainment attractors. First, we reproduce all sets of resonance attractors by feedback control of the excitability of the system as was done in the experiment. We can see that the final radius of the attractor is determined by the position of the measuring point and the time delay τ. We suggest that it is actually related to the period of the perturbations. Thus, second, in Sec. III, we try to drive the spiral wave by disturbing the excitability of the medium periodically with square waves with a certain time delay and with sinusoidal waves. In the case of parametric modulation by square waves, the results are qualitatively the same as those obtained in experiment. Then we extend the external force to a sinusoidal parametric modulation, and the system shows similar resonance drift behavior. Based on our previous work [23,24], we know that the intrinsic period and radius of spiral stable rotation are all determined by the parameters. A temporal change of parameters will let the spiral adjust between different stable circulations and induce spiral drift behavior. In Sec. IV, the corresponding kinematics model also displays these results successfully. Some concluding remarks are given in Sec. V.

II. REPRODUCTION OF RESONANCE DRIFT WITH FEEDBACK CONTROL ON EXCITABILITY

In this paper, we use the Barkley model for all the simulations:

$$\begin{aligned} \frac{\partial u}{\partial t} &= \nabla^2 u + \frac{1}{\varepsilon} u(1-u)\left(u - \frac{v+b}{a}\right), \\ \frac{\partial v}{\partial t} &= u - v. \end{aligned} \tag{2}$$

The parameter ε affects the excitability of the system.

In this and the next section our simulations are under the parameter set $a = 0.55$, $b = 0.05$, and $\varepsilon = 0.02$, which correspond to a sparse spiral wave, and we use a spiral wave rotating in the clockwise direction. The equations were investigated by an explicit Euler method with no-flux boundary conditions on a grid of 128×128 elements with $\Delta t = 0.002\,44$ s and $L = 40$. In this case, without being disturbed, the spiral wave is rigidly rotating, the rotation period is about 5.39 s ($2209\Delta t$), and the diameter of the core is 5.16 grid lengths.

Following the processes of the experiment, we chose the point (60,60) as the measuring point previously, which is about 20 grid lengths away from the spiral tip. Whenever the wave front went through this point or after some time delay τ, we changed the value of the parameter ε to 0.022 or 0.018 (corresponding to being disturbed positively or negatively) with 0.61 s ($250\Delta t$) duration. This feedback control gives a repetitive force on the excitability. Like the phenomena shown in the experiment, the parametric modulation induced a spiral wave drifting along a circular orbit centered at the measuring point [as shown in Fig. 1(b)]. In addition, with variation of the delay time, the size of the circular orbit was also varying. Figure 2 displays the relationship between the radius of the

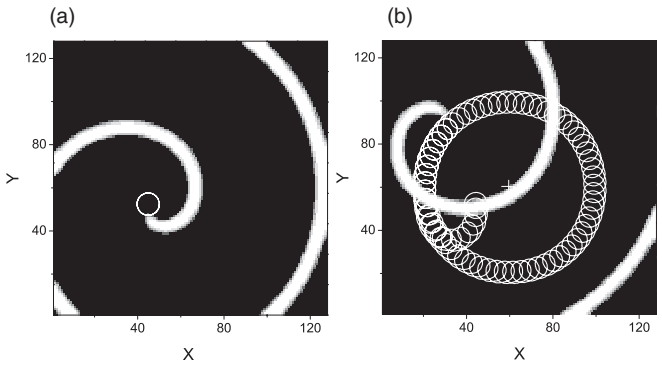

FIG. 1. Trajectories of the spiral wave tip (thin lines). (a) The initial spiral wave is rigidly rotating without being disturbed. The trajectory of its tip is a rigid circle. (b) When the spiral wave is under parametric modulation, it begins to meander along a circular pathway centered at the measuring point, which is marked by a cross. Here ε switches between 0.02 and 0.022, and the delay time is 0.

circular orbit R and the delay time τ. Qualitatively, it is the same as the result of the experiment.

A larger radius can be reached in two ways. One is by increase of the initial distance between the spiral wave tip and the measuring point d, as shown in Fig. 3. The other is by a switch in the modulation condition as was done in the experiment [19]. In Fig. 4(b), we show the trajectory of the spiral wave under the following feedback control: (1) negative disturbance, $\tau = 0$; (2) positive disturbance, $\tau =$ 750 time steps; (3) positive disturbance, $\tau = 0$; (4) negative disturbance, $\tau = 750$ time steps; (5) maintenance of the control of step 1. Each of steps 1–4 lasts for 30 000 time steps.

Obviously, the final radius of the resonance attractor is determined both by the position of the measuring point and by the time delay. But what is the crucial factor in making the radius different? We found that, when the spiral core drifts along a circular orbit stably, the period of the parameter modulation is also fixed (Fig. 5), and the period matches the only value of the radius (as shown in Fig. 6).

So we suspect that it is the period of stimulations that determines the radius R of the circular orbit, and the delay time τ only affects the choice of the adaptive period. We also can use external stimulation with a fixed period to drive the meandering

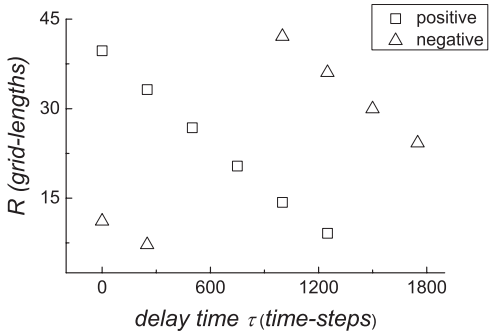

FIG. 2. variation of the radius with the delay time; the sign of the parameter changes. R vs τ plotted as squares (triangles) for positive (negative) disturbance, when ε is changed to 0.022 (0.018). The qualitative properties of the spiral drift are well consistent with the experiment.

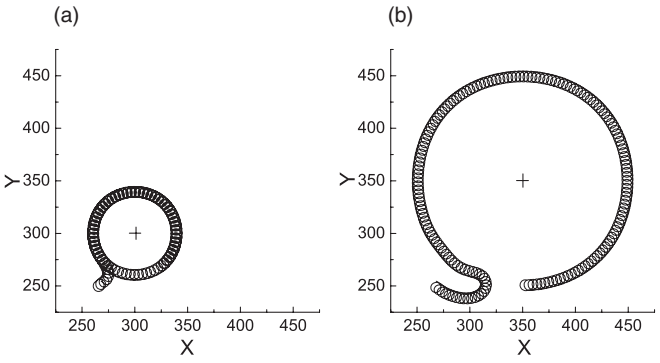

FIG. 3. Different radii of two trajectories with different initial distances d under the same feedback control. These two spiral waves are both disturbed positively, and the delay time $\tau = 0$. They are simulated on a grid of 512 × 512, with the same initial conditions. (a) The distance between the spiral tip and the measuring point (300,300) is about 56 grid lengths, and the final radius R is about 39.71 grid lengths. (b) The measuring point is (350,350), which is about 126 grid lengths far away from the spiral tip. The final radius R is about 100.26 grid lengths.

of the spiral wave, and it becomes easier to regulate the size of the circular orbit by adjusting the external period.

III. DENSE AND SPARSE SPIRAL DRIFT UNDER EXTERNAL STIMULATIONS WITH FIXED PERIOD

To investigate the relation between the radius of the circular orbit and the stable period of stimulations, we first disturbed spiral waves periodically with a square wave with a fixed period T. Within a period T, we changed the parameter ε to 0.022 or 0.018 (corresponding to positive or negative disturbance) with 0.61 s ($250\Delta t$) duration, and then reset it back to $\varepsilon = 0.02$. It turns out that the spiral core drifts along a circular path, as the experiment shows, and the radius is the same as what is observed in simulation of the experiment with feedback control (see Fig. 6).

For the feedback control, the period of disturbance is determined by the movement of the spiral wave itself. It is always larger than the intrinsic period of the original spiral wave. Otherwise, unlike the feedback control, when we disturb the spiral wave directly with a periodic function, the period of disturbance can be set at any value. Thus, by forcing the

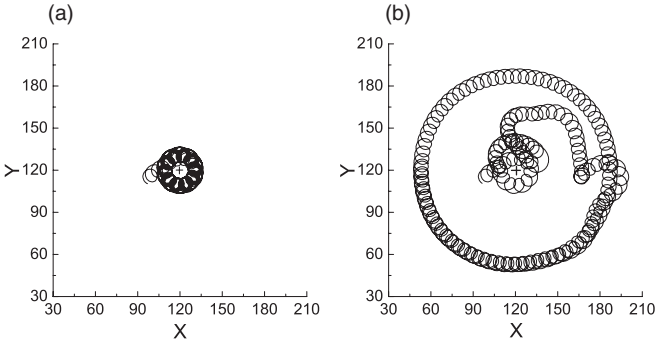

FIG. 4. (a) Negative disturbance, $\tau = 0$, $R = 11.09$ grid lengths. (b) Through a sequence of control method transitions, the radius reaches a larger one, $R = 67.39$ grid lengths.

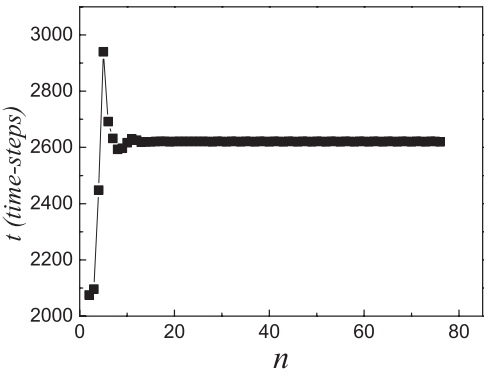

FIG. 5. Time interval t (measured by time steps) before each stimulation. It reaches a fixed value after several periods of modulation. Here the stimulation is negative with delay time $\tau = 250$.

spiral wave with periodic functions, we can get more drifting behaviors than with feedback control, especially in the cases where the disturbing period is less than the intrinsic period of the spiral (as shown in Fig. 7).

For a wide range of forcing periods, there are always resonance attractors for spiral wave drift. However, the spiral wave changes its rotation direction once when the forcing period pass a critical value. In Fig. 7, the hollow triangles representing its trajectories are epicycloids, whereas the solid triangles represent hypocycloid trajectories, and each of these two lines follows an exponential function. The results show clearly the existence of a critical disturbance period and full resonance drifts. We have also tried the same numerical simulation for a dense spiral wave with $a = 1.0$, $b = 0.03$, and $\varepsilon = 0.02$ (the parameter sets for a dense spiral wave are all the same in this paper); the results are the same qualitatively.

Furthermore, based on the above approach, we may just as well change the parameter ε continuously and periodically, by using a sinusoidal function:

$$\varepsilon(t) = 0.021 + 0.001\sin\left(\frac{2\pi t}{T}\right). \tag{3}$$

With a change of the period T, the results for resonance drift are similar to those obtained by periodic disturbances by square

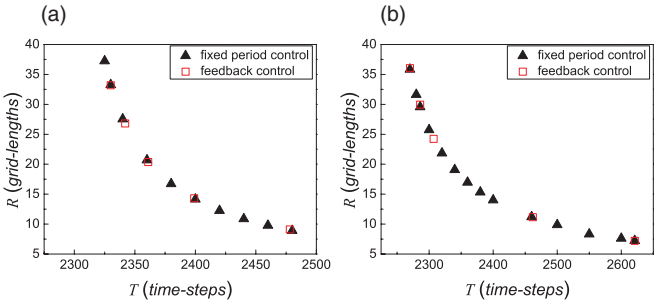

FIG. 6. (Color online) Radius R corresponding to the stable modulation period for positive (a) and negative (b) disturbance. The hollow squares are the results observed in the experimental simulation of feedback control, while the solid triangles present the results of a simulation with fixed period T modulation. There is a critical point of T. When T is near this critical point, the radius R tends to infinity. When T is too large, the resonance attractor is not observed.

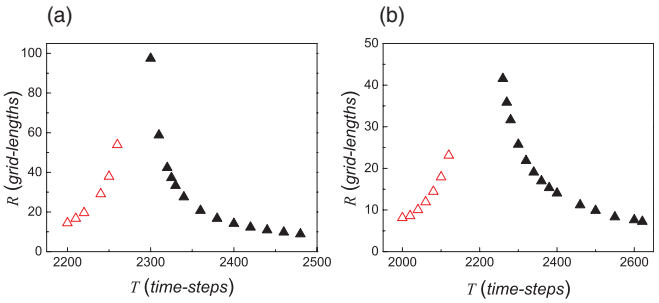

FIG. 7. (Color online) For a sparse spiral wave, the radius R changes with the external forcing period T on both positive (a) and negative (b) disturbances. The red open triangles represent the epicycloidal trajectories, while the filled triangles represent the hypocycloidal trajectories.

waves (as shown in Fig. 8). Furthermore, the drift behavior of a dense spiral wave [Fig. 8(a)] does not have qualitative differences from that of a sparse spiral wave [Fig. 8(b)].

IV. A KINEMATIC MODEL FOR THE RESONANCE DRIFTS OF A SPIRAL WAVE

We know that the intrinsic period and radius of a spiral stable rotation are all determined by the parameters. A spatial or temporal change of parameters will let the spiral adjust between different stable circulations and induce the spiral drift behavior. In previous studies, we developed a kinematic model for spiral wave drift [23,24], which can well capture the different drifting behaviors of dense and sparse spiral waves in the same conditions. In the present study, we apply this model to periodic disturbances, when the parameter ε is a sinusoidal function of time.

We describe the tip motion using the following differential equations:

$$\begin{aligned} \dot{x} &= c_g \cos\theta - h c_n \sin\theta, \\ \dot{y} &= c_g \sin\theta + h c_n \cos\theta, \\ \dot{\theta} &= h\omega, \end{aligned} \tag{4}$$

where h is the chirality of the vortex ($h = +1$ for counterclockwise and $h = -1$ for clockwise rotation).

When the spiral is in stable circulation, the dependence of the core radius R_c and rotation period P_c on the parameter ε,

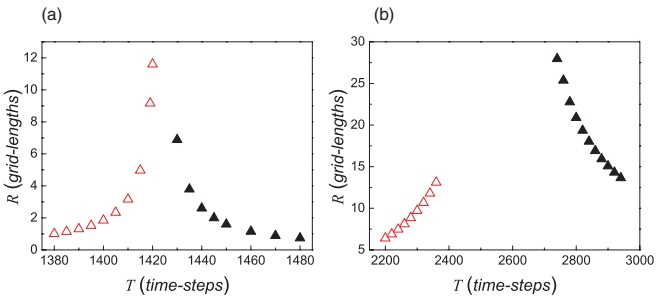

FIG. 8. (Color online) The radius R vs the period T for a dense spiral wave (a) and a sparse spiral wave (b), when the parameter changes following the trigonometric function Eq. (3). The red open triangles represent the epicycloidal trajectories, while the filled triangles represent the hypocycloidal trajectories.

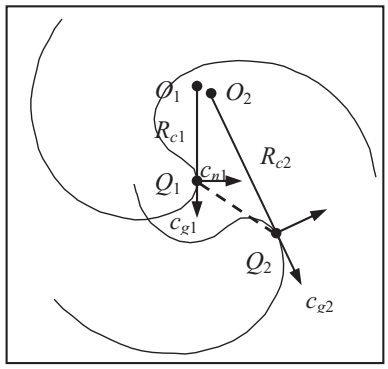

FIG. 9. A schematic diagram of spiral drift.

i.e., $R_c = R_c(\varepsilon)$ and $P_c = P_c(\varepsilon)$, can be obtained by numerical simulation. For the dense spiral wave, both R_c and P_c increase almost linearly with ε; we fit them by

$$\begin{aligned} R_c &= (0.365 + 13.235\varepsilon) \times 40/128, \\ P_c &= 1.78 + 80.84\varepsilon. \end{aligned} \tag{5}$$

For the sparse spiral wave, both R_c and P_c increase with ε nonlinearly, and we fit them by

$$\begin{aligned} R_c &= (-0.62e^3 + 0.9e^5\varepsilon - 4.6e^6\varepsilon^2 + 0.75e^8\varepsilon^3) \times 40/128, \\ P_c &= -596.5 + 8.8e^4\varepsilon - 4.3e^6\varepsilon^2 + 7.2e^7\varepsilon^3. \end{aligned} \tag{6}$$

Since the sparsity of the spiral wave is due to low excitability of the medium, the diameter and cycle length of the sparse spiral wave are larger than those of the dense spiral wave.

The conduction velocity of the spiral tip Q satisfies $V_c(\varepsilon) = 2\pi R_c(\varepsilon)/P_c(\varepsilon)$. Just like the core radius, the rotation period and the conduction velocity are functions of the parameter ε; when the spiral wave is subjected to external periodic forcing, they will be changed accordingly and induce the resonance drifting behavior. As shown in a schematic diagram of spiral drift in Fig. 9, a change of the above quantities will lead to a change of the normal velocity of the spiral tip, c_n, the instantaneous rotation period P, and the instantaneous angular velocity ω, and lead to the additional radial velocity c_g. Thus, when the system is disturbed with a continuous periodic function subject to the parameter ε, we assume that these quantities obey the following equations:

$$c_n(\varepsilon) = V_c(\varepsilon) + \lambda \Delta V_c = V_c(\varepsilon) + \lambda V_c'(\varepsilon)\varepsilon'(t), \tag{7}$$

$$P(\varepsilon) = P_c(\varepsilon) + \gamma \Delta P_c = P_c(\varepsilon) + \gamma P_c'(\varepsilon)\varepsilon'(t), \tag{8}$$

$$c_g(\varepsilon) = \rho \Delta R_c - \alpha \Delta V_c = (\rho R_c' - \alpha V_c')\varepsilon'(t), \tag{9}$$

$$\omega = \frac{2\pi}{P} - \beta \frac{c_g}{c_n}, \tag{10}$$

where (and in the following formulas) a prime on R_c, V_c, and P_c means their derivatives with respect to the parameter ε. λ, γ, ρ, α, and β are adjustable parameters. In this paper, we use the trigonometric function (3) to disturb the system. So the parameter ε is time dependent as in Eq. (3), and its derivative

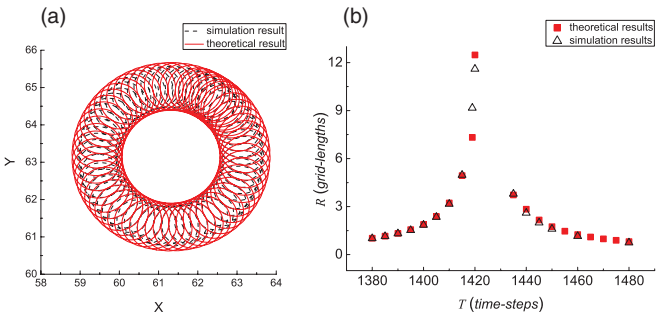

FIG. 10. (Color online) Drifting behaviors of a dense spiral wave from simulation and the kinematical model for the same initial conditions. The external period $T = 1400$ is shown in (a). The parameter sets for the kinematic model are $\lambda = 1.56$, $\gamma = 0.8$, $\rho = 2.73$, $\alpha = 1.56$, and $\beta = 0.003$.

is

$$\varepsilon'(t) = 0.001\frac{2\pi}{T}\sin\left(\frac{2\pi t}{T}\right). \tag{11}$$

Combining Eqs. (7)–(11), one can obtain the spiral wave drift behaviors. For example, Fig. 10(a) shows the tip trajectory of a dense spiral wave and the corresponding result from the kinematic equations with the external period $T = 1400$, and Fig. 10(b) shows their radii corresponding to the external periods. While the Fig. 11 shows the results for a sparse spiral wave. They all show a very good agreement.

V. CONCLUSION

In previous research on spiral wave dynamics under an external force, especially in the light-sensitive BZ reaction, the effects are usually described via the periodic modulation of the term ϕ in the Oregonator model, which represents the light-induced flow of Br^-. In this paper, a more general approach, that is, modulation of the system excitability, is suggested. It is revealed that it can produce qualitatively the

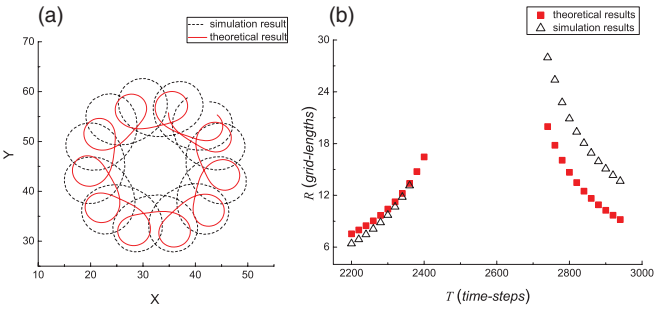

FIG. 11. (Color online) Drifting behaviors of a sparse spiral wave from simulation and the kinematical model for the same initial conditions. The external period $T = 2340$ is shown in (a). The parameter sets for the kinematic model are $\lambda = 0.6$, $\gamma = 0.1$, $\rho = 3$, $\alpha = 6$, and $\beta = -3$.

same phenomenon of resonant drifting of the spiral wave. This approach provides us a more general perspective to investigate the effects of external forces. Thus, in addition to the light-sensitive BZ reaction, the forced dynamics of spiral waves in many other excitable media can also be investigated in this approach. Furthermore, it is found that the radius of the circular orbits of resonance drift is determined only by the period of the external forces. Then the drift of dense and sparse spiral waves is given under external stimulations with fixed period, i.e., with square wave and sinusoidal functions. With change of the forcing period, the trajectory of the spiral wave changes from an epicycloid to a hypocycloid (the spiral rotates in the clockwise direction). Between these two phases, there is a certain value of T at which the spiral core drifts in a straight line. Moreover, these results can be calculated through our kinematical model very well. This demonstrates again that kinematical considerations can well capture the drifting dynamics observed in reaction-diffusion equations.

[1] A. M. Zhabotinsky and A. N. Zaikin, *Oscillatory Processes in Biological and Chemical Systems*, Vol. 2 (Nauka, Pushchino, Russia, 1971).
[2] A. T. Winfree, Science **175**, 634 (1972).
[3] F. Siegert and C. J. Weijer, Physica D **49**, 224 (1991).
[4] S. Jakubith, H. H. Rotermund, W. Engel, A. von Oertzen, and G. Ertl, Phys. Rev. Lett. **65**, 3013 (1990).
[5] A. T. Winfree, Chaos **8**, 1 (1998).
[6] A. Garfinkel, Y.-H. Kim, O. Voroshilovsky, Z. Qu, J. R. Kil, M.-H. Lee, H. S. Karagueuzian, J. N. Weiss, and P.-S. Chen, Proc. Natl. Acad. Sci. USA **97**, 6061 (2000).
[7] J. M. Davidenko, A. M. Pertsov, R. Salomonsz, W. Baxter, and J. Jalife, Nature (London) **355**, 349 (1992).
[8] H. Zhang, Z. Cao, N.-J. Wu, H.-P. Ying, and G. Hu, Phys. Rev. Lett. **94**, 188301 (2005).
[9] G. Hu, J. Xiao, L. O. Chua, and L. Pivka, Phys. Rev. Lett. **80**, 1884 (1998).
[10] W. Liu, J. Xiao, and J. Yang, Phys. Rev. E **72**, 057201 (2005).
[11] Q. Ouyang and H. L. Swinney, Nature (London) **352**, 610 (1991).
[12] A. T. Winfree, Phys. Lett. A **149**, 203 (1990).
[13] A. T. Winfree, Physica D **49**, 125 (1991).
[14] X. Zhang, M. Fu, J. Xiao, and G. Hu, Phys. Rev. E **74**, 015202 (2006).
[15] J. Lee, J. Kim, G.-h. Yi, and K. J. Lee, Phys. Rev. E **65**, 046207 (2002).
[16] S. Grill, V. S. Zykov, and S. C. Müller, J. Phys. Chem. **100**, 19082 (1996).
[17] V. S. Zykov, O. Steinbock, and S. C. Müller, Chaos **4**, 509 (1994)
[18] S. Grill, V. S. Zykov, and S. C. Müller, Phys. Rev. Lett. **75**, 3368 (1995).

[19] On-Uma Kheowan, Vladimir S. Zykov, Orapin Rangsiman, and Stefan C. Müller, Phys. Rev. Lett. **86**, 2170 (2001).
[20] A. Karma and V. S. Zykov, Phys. Rev. Lett. **83**, 2453 (1999).
[21] V. S. Zykov, G. Bordiougov, H. Brandtstadter, I. Gerdes, and H. Engel, Phys. Rev. E **68**, 016214 (2003)
[22] V. S. Zykov, O. U. Kheowan, O. Rangsiman, and S. C. Müller, Phys. Rev. E **65**, 026206 (2002).
[23] Z. Di, Z. Qu, J. N. Weiss, and A. Garfinkel, Phys. Lett. A **308**, 179 (2003).
[24] L. Xu, Z. Qu, and Z. Di, Phys. Rev. E **79**, 036212 (2009).